Microstructure, mechanical and fractographic behaviour of the diffusion welded joints of AA2219 and Ti-6Al-4V for aerospace applications

Manjunath Vatnalmath, V Auradi
Dept. of Mechanical Engineering, Siddaganga Institute of Technology, Tumakuru-572103, Visvesvaraya Technological University Karnataka, India
vmanjunathsit@gmail.com, https://orcid.org/0000-0003-3138-9453
vsauradi@gmail.com, http://orcid.org/0000-0001-6549-6340

Bharath V, Anirudh Bharadwaj, Chethan Gowda
Department of Mechanical Engineering, RNS Institute of Technology, Bengaluru-560098, Visvesvaraya Technological University Karnataka, India
bharathv88@gmail.com,http://orcid.org/0000-0001-6765-4728, anirudhb425@gmail.com, chethanvgowda27@gmail.com

Madeva Nagaral
Configuration and Mass Properties, Aircraft Research and Design Centre, Hindustan Aeronautics Limited, Bangalore 560037, Karnataka, India,
madev.nagaral@gmail.com, http://orcid.org/0000-0002-8248-7603

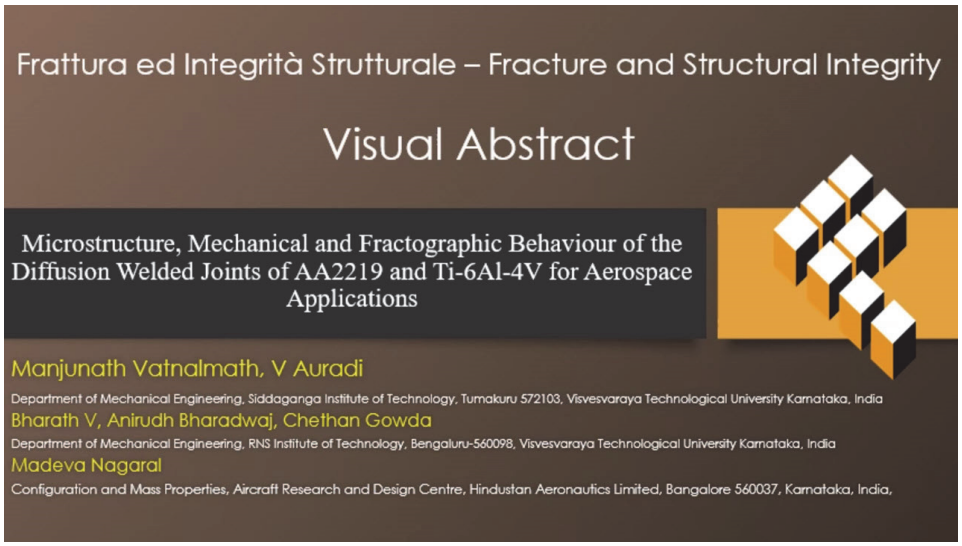

Citation: Vatnalmath, M., Auradi, V., Bharath, V., Bharadwaj, A., Gowda, C., Nagaral, M., Microstructure, Mechanical and Fractographic behaviour of the Diffusion Welded Joints of AA2219 and Ti-6Al-4V for Propellant Tank Applications, Fracture and Structural Integrity, 71 (2025) 37-48.

Received: 26.06.2024
Accepted: 04.10.2024
Published: 08.10.2024
Issue: 01.2025

KEYWORDS. AA2219, Diffusion welding, Microstructure, Interface, Intermetallic, Brittle fracture.

INTRODUCTION

Regarding the sustainable utilization of outer space, prominent spacefaring nations and international organizations have suggested a range of measures to mitigate space debris, such as the intentional descent of spacecraft upon their operational lifespan. To mitigate the increased risk of ground casualties caused by more frequent re-entry of

objects, it is possible to build a spacecraft using a philosophy that prioritizes its demise during re-entry, resulting in most of the spacecraft not surviving the process. These tactics may prioritize uncontrolled disposal options for re-entry over regulated ones, as they increase the likelihood of meeting the standards for minimizing the danger of casualties [1]. The Design for Demise (DFD) implemented by the European Space Agency (ESA) in 2008 stipulates that any object launched into space must completely burn or ablate while reaching the Earth's atmosphere upon re-entry or failure. Titanium (Ti) alloys are used in propellant tanks significantly due to their excellent properties, such as high strength-to-weight ratio, high corrosion resistance, and good congruity with nearly all propellants. However, it has a high melting point of about 1600°C, which is in the range of the highest temperature that may be experienced by any space object upon re-entry. It is a significant risk factor that some components of the propellant tanks would remain unburnt and cause ground casualties and other possible destructions. Henceforth, it is vital to discover a substitute material for titanium in the fabrication of the components of the propellant tank like transition rings and tubings. Moreover, there is a need of joining aluminium (Al) with titanium (Ti) to enhance the functional properties and reduce the weight. Aluminium alloy (AA) 2219 is presently used to fabricate cryogenic tanks and it is a notable material due to its good resistance to corrosion cracking, high specific strength, and excellent ductility at cryogenic temperatures. In parallel, the cost and weight reduction by not compromising adequate performance have become crucial in the aerospace industry. There are various strategies to fulfill these requirements. It is widely recognized that welding is increasingly replacing the traditional method of using rivets for fuselage structures. Another highly efficient option is the utilization of hybrid constructions, where components composed of diverse materials can be customized to meet specific local requirements. There is a need for a welding technology that can efficiently join different materials, such as titanium and aluminium. The joining of aluminium and titanium will benefit the pipework, tubing and liner surrounding the propellant tank [2, 3].

The fusion welding process in aerospace has been limited due to high susceptibility to cracks in welded joints, which can compromise structural integrity, and the limited ability to weld aluminium alloys, especially the 2xxx and 7xxx series that are increasingly used in airframes, fuel tanks of launch vehicles, space shuttles, and spacecraft [4]. As a result, many advanced and expensive welding techniques like electron beam welding, laser beam welding, and friction welding are implemented due to their advantages over fusion welding in joining aluminium and titanium alloys. However, these methods face difficulties in overcoming the porosities, cracks, and presence of debris [5] in the diffusion zone. In addition, the lower welding reliability of Al alloys due to high thermal conductivity, high reflectivity, low viscosity and the substantial differences in thermal and metallurgical properties between the Al and Ti makes these welding methods challenging. [6]. Other suitable welding techniques, like Tungsten inert gas (TIG) welding of Al and Ti alloys, produce metallurgical defects in the fusion zone, thereby decreasing the tensile strength of the joints. Explosive welding can reach a temperature of up to 2100 K, which causes the aluminium and titanium to melt and furthermore generates residual stresses and increases the density [7]. Recently, vacuum diffusion welding has been employed in joining dissimilar metals with low heat input conditions, where the temperature is significantly below the melting point of the base metal without generating metallurgical defects and retaining the base metal properties. Moreover, vacuum diffusion bonding offers the benefits of no macroscopic plastic deformation and consistent interfacial structure and excludes the requirement for post-welding processing.

In the diffusion welding method, the two joining surfaces are stacked together at a temperature of about 0.7-0.9 times the absolute melting temperature of the base metal and an optimum pressure which does not create macroscopic deformation performed for an adequate holding time to form a bonding joint. Further, the bonding process does not develop a fusion zone, reducing the chance of forming residual stresses at the welding joint [8-9]. Diffusion welding of Al to Ti alloys is challenging due to the high oxide stability and moderate oxygen solubility of Al at elevated temperatures, causing difficulties for diffusion welding due to its detrimental impact on atom diffusion, leading to a relatively weak joint. Therefore, it is imperative to chemically purify the surface of the aluminium before the diffusion welding. Contrarily, Ti exhibits a notable capacity to dissolve oxygen, and the stable oxide gradually dissolves at elevated temperatures [10]. In the context of the difficulties discussed, few investigations are carried out on the solid-state diffusion welding of Al and Ti alloys. Some of the studies obtained good bonding at the temperature near the solidus temperature of the Al alloys with optimum pressure and holding times [11, 12]. However, some other studies used very high temperatures close to the melting point of Al alloys for a longer holding time. In addition, it is noted that the formation of the intermetallic phases Al_3Ti is inevitable, and the fracture generally occurs at the interface of Al_3Ti and Al, which will have a major impact on the bonding strength of the welded joints [13-15]. The current study aims to investigate the microstructure and mechanical properties of the diffusion welded AA2219 and Ti-6Al-4V alloys. Furthermore, the bonding strength of the welded joints, hardness, and intermetallic formation across the interface are evaluated.

EXPERIMENTAL DETAILS

Materials and methods

The received base metals, AA2219 and Ti-6Al-4V alloys, are machined to the dimensions of 50×50×5 mm3 using wire electric discharge machining (EDM). Chemical composition of the base metals is analyzed by an optical emission spectrometer (BAIRD-DV6). Tab. 1 shows the elemental composition of the base metals AA2219 and Ti-6Al-4V. Subsequently, the machined samples are polished using different grade SiC grits in the range 220-1200. Mechanically ground samples are tested for the surface roughness using Talysurf instrument and the surface roughness values (Ra) of 0.211 µm and 0.045 µm are observed on aluminium and titanium surface respectively. The faying surfaces are chemically washed with 6% NaOH and 40% HNO3 to inhibit the oxide formation and further cleaned in an acetone bath for 10 minutes before the diffusion welding and kept in the vacuum bonding furnace in a stacked manner. A schematic illustration of the bonding furnace, base metals and shear test specimen placed in a fixture for bond strength evaluation is shown in Fig. 1.

Base Metals	Elements (wt %)										
	Ti	Mg	C	Si	Fe	Zr	Mn	Cu	Zn	V	Al
AA2219	0.06	0.01	-	0.49	0.23	0.2	0.32	6.48	0.18	0.06	Bal.
Ti-6Al-4V	Bal.	-	0.056	-	0.29	-	-	-	-	3.75	5.68

Table 1: Chemical composition of base metals

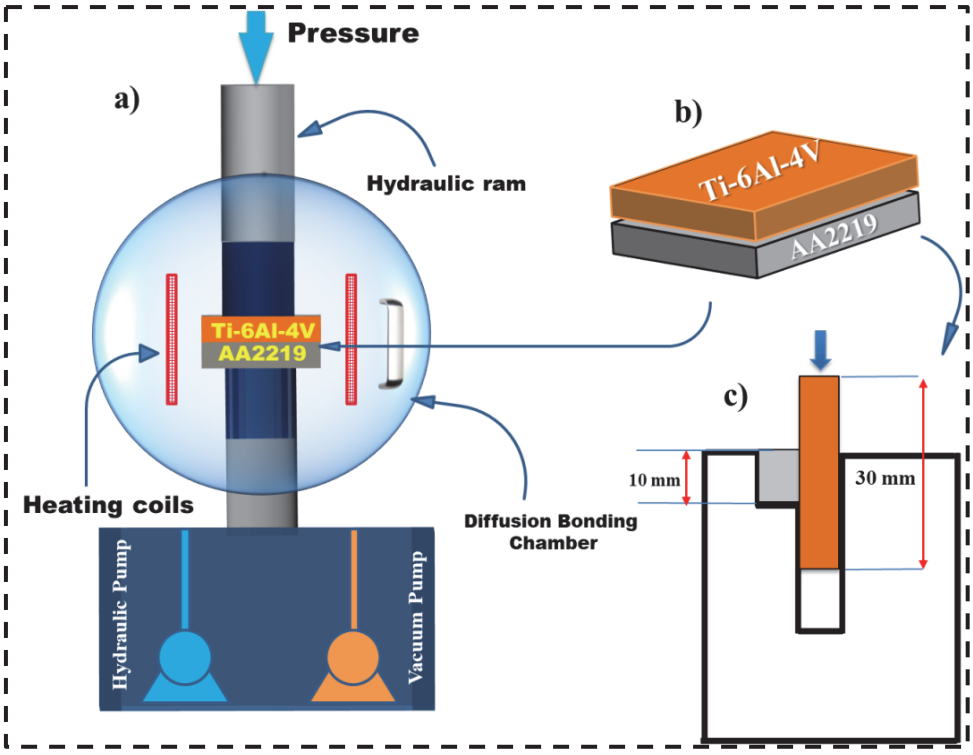

Figure 1: Schematic illustration of a) Bonding furnace b) base metals c) shear test specimen placed in a fixture

The diffusion welding is carried out by controlling the vacuum to $7x10^{-4}$ Torr, and the temperature is increased gradually to 540°C. The process consists of 30 minutes of ram time and 10 minutes of soaking time for each step in temperature rising, as shown in the process cycle (Fig.2). Once the optimum temperature is reached, the bonding pressure of 4MPa is applied for the holding periods of 30, 60, 90, and 120 minutes. The variables are programmed using a control panel attached to the vacuum bonding furnace. The temperature, pressure, and range of holding times are preferred based on

previous studies and economic factors for the sustainable production of dissimilar diffusion welding joints. The diffusion welding method needs longer holding time than other solid-state welding methods to ensure intimate contact, improve joint quality, void closure and improve grain growth across the interface [16]. However, when the creep phenomenon starts at an elevated temperature, the longer holding time makes it difficult to control the macroscopic plastic deformation. It would also be detrimental to the diffusion of atoms and metallurgical purity at the joint areas as the longer holding time increases the chance of forming brittle intermetallics. Henceforth, the present study adheres to the holding time in the range of 30 to 120 minutes. After the diffusion welding, the samples are cut perpendicularly to the welding joint using wire EDM for microstructure and shear strength (Fig. 1c) evaluation. The specimens are then polished using different SiC grit papers (220-2000) and grounded using a diamond suspension of 1μ. Polished samples are then cleaned ultrasonically in an acetone bath and dried using hot air. The cleaned samples are etched with Keller's reagent for the Al side and Kroll's reagent for the Ti side to evaluate the microstructure and elemental composition at the bonding interface using SEM, EDS (Zeiss Gemini ULTRA 55), and XRD (Rigaku SmartLab) with 1.542 Å (Cu K-α) and step size of 2°/min is used to identify the intermetallic compounds formed at the interface of the diffusion welded joints. Shear strength (BISS-25 kN) is evaluated using a customized shear fixture under ambient temperature and a cross head speed of 1 mm/min. The hardness of the bond interface is assessed using Vickers microhardness (MICROMACH) for an indentation load of 50 g and a dwell period of 15 sec.

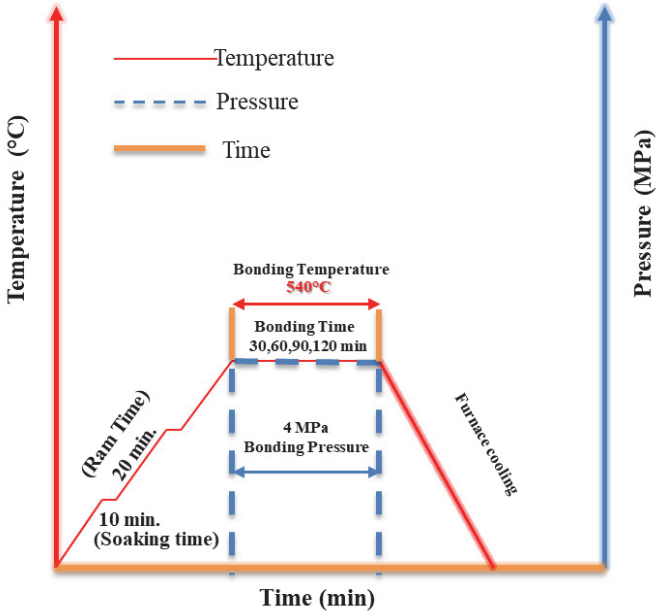

Figure 2: Temperature-pressure-time curve for the current diffusion welding process.

RESULTS AND DISCUSSION

Joint Microstructure

Fig.3 shows BSE (back scattered electron) micrographs of the specimens diffusion welded at holding time in the range of 30-120 minutes. The bonding line of the specimen welded at 30 minutes (Fig. 3a) shows irregular and elliptical voids at the interface zone. The point EDS analysis is carried out on the bonding line, shown in Tab. 2. Point 1 (Fig.3a) on the interface of the diffusion welded joint at 30 minutes has 85.76 at% Al and 14.24 at% of Ti, which specify the formation of the α-Al (Al-rich zone) with a small amount of Ti. During diffusion welding, the bonding surfaces undergo a plastic deformation process. This process involves crushing surface asperities, which are small irregularities on the surface, under axial stress when loaded. The purpose of this deformation is to fill the interfacial gaps between the surfaces, leaving behind residual voids [17]. However, an adequate holding time is necessary for the further closure of voids. When the holding time is increased to 60 minutes, the bonding interface exhibits spherical voids, and a diffusion layer or a reaction layer of 0.5 μm is formed near the Ti. The Kirkendall effect causes the formation of small spherical voids near the Al-rich interface as the diffusion coefficient of aluminium in titanium is generally between $3x10^{-14}$ to $1.2x10^{-13}$ m^2/s and that of titanium in aluminium is 5.0×10^{-18} to 3.5×10^{-17} m^2/s at the temperature range of 530-600°C

[18]. The voids formed act as atomic diffusion paths to form a diffusion layer and the net movement of atoms is directed towards the Al-rich layers, causing the interface to move away from the Al-rich layers and towards the Ti-rich layers. The diffusion welded specimen at 90 minutes shows minute voids on its interface. A diffusion layer of 1.1 μm is formed near the Ti interface, and EDS on the joint interface (Fig.3c) constitutes 62.44 at% of Al of and 37.56 at% of Ti. The diffusion welded joint at 120 minutes (Fig.3 d) shows the formation of a thick diffusion layer of 3.8 μm without exhibiting voids at the interface. However, the plastic deformation at the Al interface is evident, which further signifies the effect of higher holding time. The point EDS (Fig.3d) on the interface has 58.2 at% of Al and 41.8% of Ti, specifying the formation of $TiAl_3$. In addition, the Al-Ti binary phase diagram could predict the formation of intermetallic compounds for the different elemental composition that exists at the interface of the joints [19].

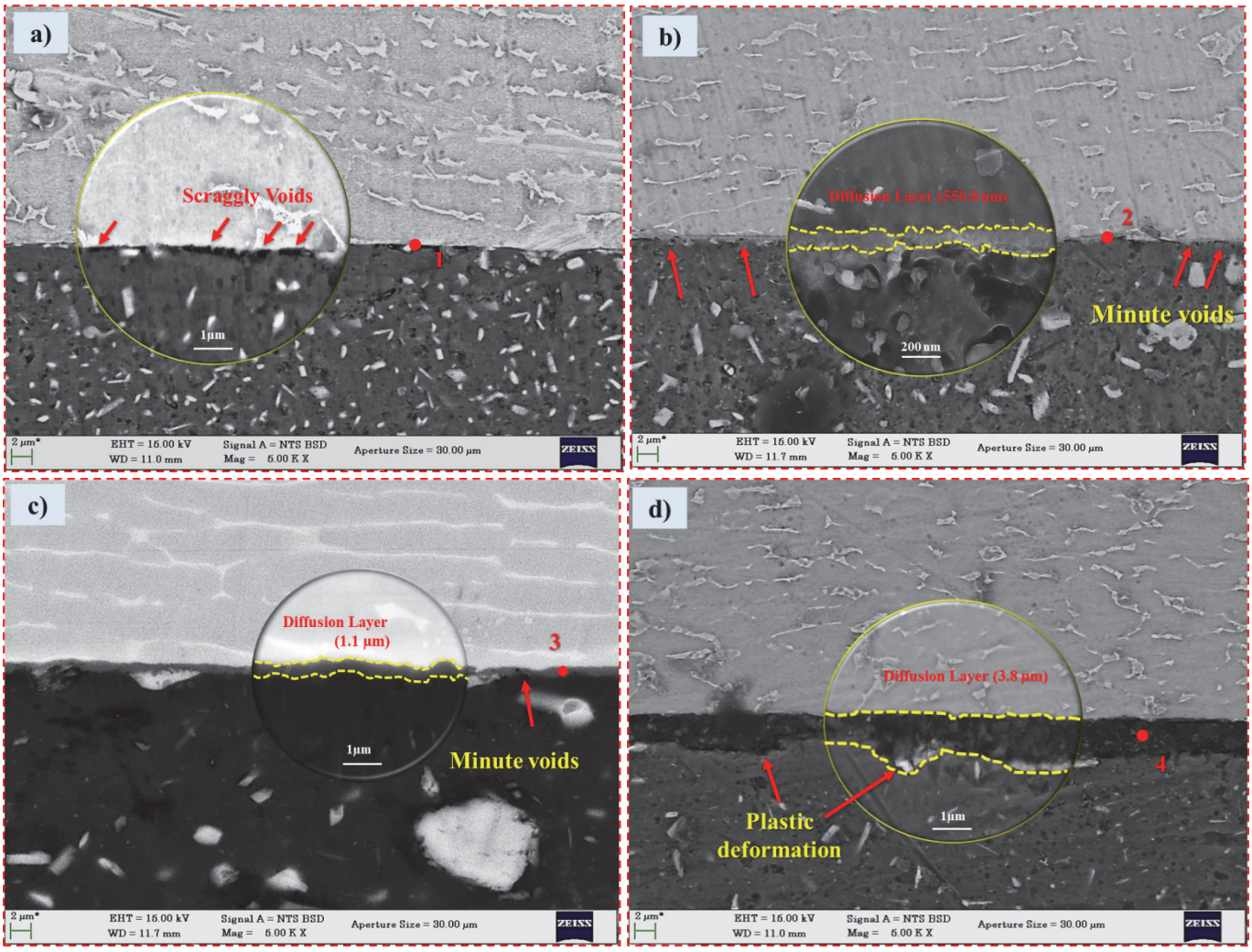

Figure 3: BSE micrographs of the diffusion joints welded at a) 30 b) 60 c) 90 and d) 120 minutes

Point Number	Elements (at %)	
	Al	Ti
1	85.76	14.24
2	71.08	28.92
3	62.44	37.56
4	58.20	41.80

Table 2: EDS analysis on the points illustrated in Fig.3.

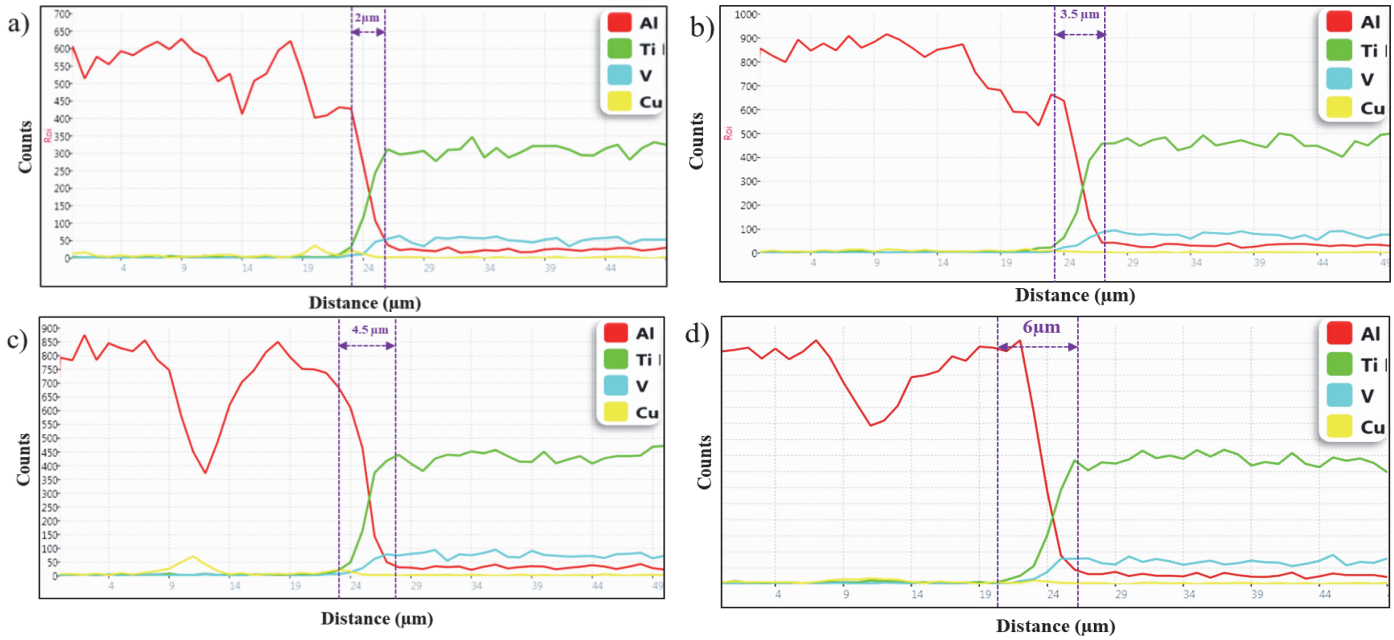

Figure 4: Line scan EDS results for the joints welded at a) 30 b) 60 c) 90 and d) 120 minutes

The diffusion behaviour further analyzed by the line scan EDS across the interface of the diffusion welded joints at various holding times, shown in Fig. 4. The line scan across the joint formed at 30 minutes shows diffusion between the Al and Ti, which exhibits a diffusion zone of 2 µm (Fig.4a) without showcasing a diffusion layer towards Ti (Fig.3a). Further the joints formed at 60, 90 and 120 minutes imparts a strong diffusion across the interface of the Al and Ti and exhibits a diffusion zones of 3.5, 4.5 and 6 µm respectively. However, the increase in holding time above a specific limit may cause metallurgical deterioration of the parent metal interface (Fig. 3 d) due to the thermal degradation of the precipitates, which further causes the formation of brittle intermetallics and incoherent precipitates. In addition, elevating the holding time leads to variability in the diffusion of the contacting metals and forms only a secondary phase at the interface rather than eliciting the interface of the base metal [20]. The effect of higher holding time is evident for the joint formed at 120 minutes (Fig. 3d). The interface clearly specified the formation of brittle phase and the metallurgical difference in the reaction layer formed at the interface in comparison to the diffusion welded joints at 60 and 90 minutes can be observed. The resulting diffusion zones (Fig.4) are further considered as the specific regions accountable for forming the different intermetallic compounds.

Fig. 5 shows the plotted curve for diffusion zone thickness against the square root of holding time at 540°C. The results elucidate that the thickness of the diffusion zone is confirmed to have a linear relationship with the square root of holding time with a linear fitting coefficient of R^2= 0.98. In addition, it is evident that the growth of the reaction layers between the Al and Ti is diffusion controlled phenomenon. In diffusion welding, the relationship between the formation of the diffusion layer at the interface and the holding time for the 540°C follows a parabolic growth law which is expressed below in Eqn. 1 [21].

$$x = k\sqrt{t} \tag{1}$$

where, x is the thickness of the diffusion zone, t is the holding time and k is the growth rate constant.

Microhardness

The microhardness profile across the interface of the diffusion welded joints is shown in Fig.6. The Vickers microhardness method is used to analyze the variation in microhardness at the joints produced at 30, 60, 90, and 120 minutes by applying an indentation load of 50 g. The diffusion welded specimen at 30 minutes exhibits a hardness value of 91.3 $HV_{0.05}$ at its joint. Further, the hardness at the joints is increased with an increase in the holding time due to the closure of interfacial cracks, voids and the formation of intermetallic compounds at the interface zone. The hardness of 174 and 186 $HV_{0.05}$ is observed on the joints bonded at 60 and 90 minutes, respectively. However, the joint formed at 120

minutes demonstrates a much higher hardness of 202.5 $HV_{0.05}$ owing to the presence of brittle intermetallic phases at the joint interface (Fig.3d). The formation of a diffusion layer at the joint interface results in an increase in hardness at the joints compared to the hardness at the aluminium side. The average hardness of 65 $HV_{0.05}$ on the aluminium side and 425 $HV_{0.05}$ on the titanium side are obtained.

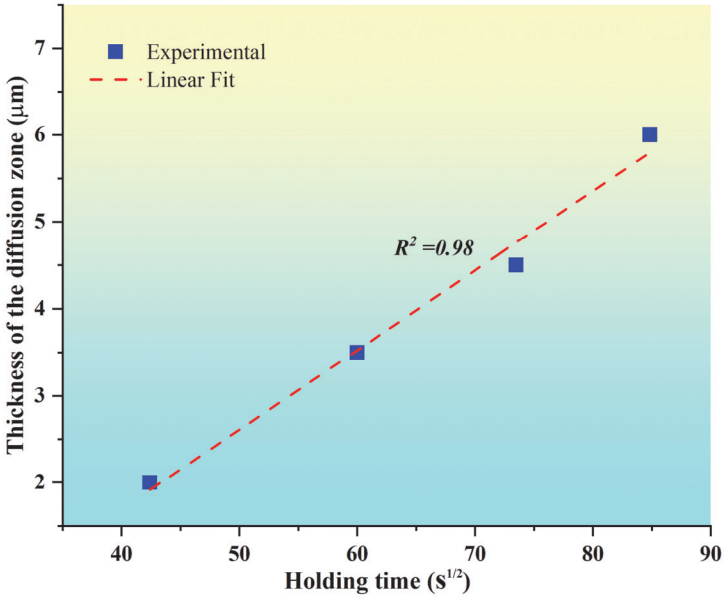

Figure 5: Thickness of the diffusion zone as a function of the square root of holding time for 540°C.

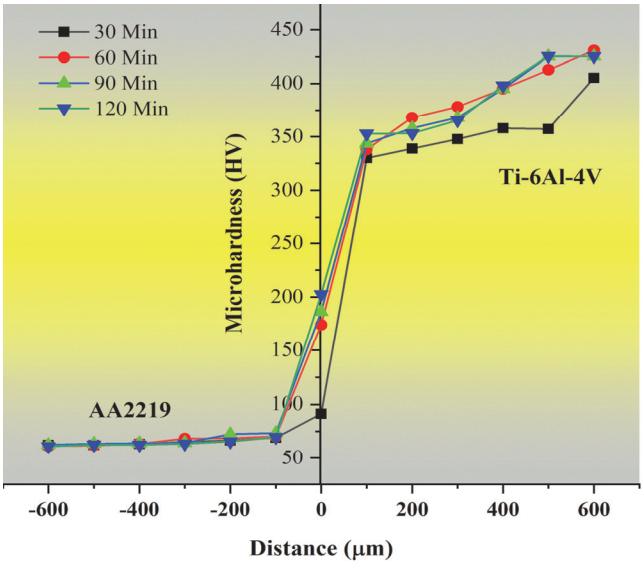

Figure 6: Microhardness profile for the joints formed at various holding times

Shear strength

Fig.7 (a) and Fig. 7 (b) illustrate the load against the displacement curve and the shear strength as a function of holding time, respectively. The joint produced at 30 minutes exhibited a lower shear strength value of 49 MPa, pertaining to the presence of voids along the bonding line and inadequate bond quality. Furthermore, shear strength of 78.4 MPa and 143.58 MPa is observed for the joints produced at 60 and 90 minutes, respectively. However, when the holding time increased to 120 minutes, the shear strength gradually decreased and attained a value of 133.8 MPa. During longer holding periods, the plastic deformation of mating surfaces becomes more apparent compared to shorter bonding periods. As the bonding duration increases, the bond strength steadily decreases due to an increase in the thickness of intermetallics around the bond interaction. Shear strength has an inverse relationship with holding time and the extended time required for diffusion is also a reason for the insignificant secondary effects in complex alloys [22]. However, the resulting shear

strength of the diffusion welded joint at the holding time of 90 minutes is evidently high compared to the study carried out on the diffusion bonding of AA7075 and pure Ti [15].

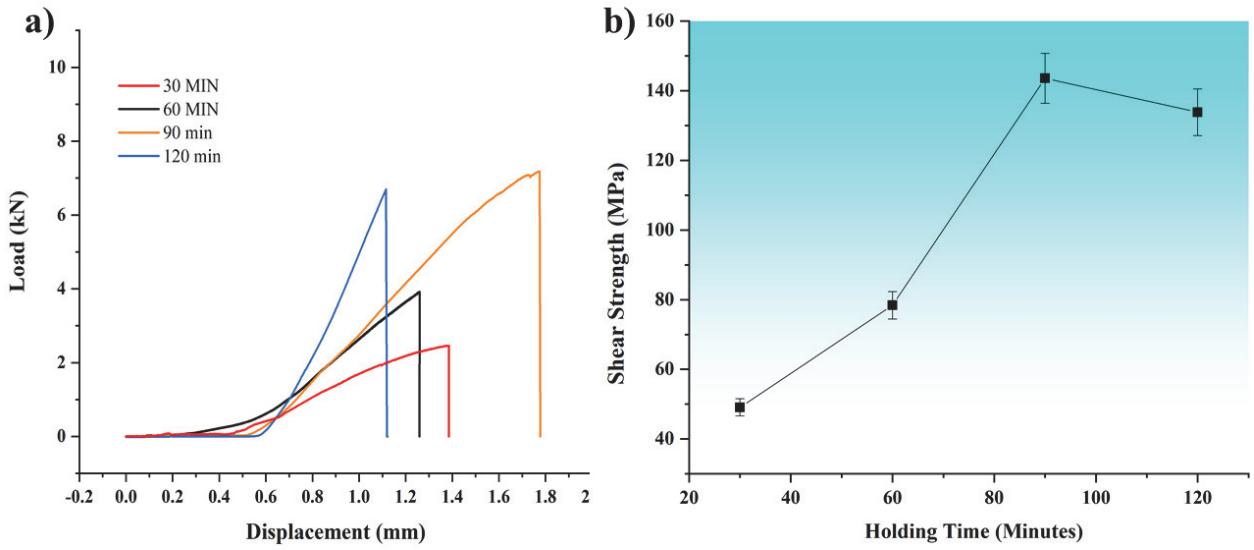

Figure 7: Shear strength results of the diffusion welded joints a) load vs. displacement curve b) shear strength as a function of holding time.

Fracture morphology

Fractography analysis of the diffusion welded joints formed at various holding times in the range of 30-120 minutes is shown in Fig.8. The joints predominantly fail at the bonding line as the compressive load is applied normally the joint section. The fractured surfaces of the specimen formed at the holding time of 30 minutes exhibit a peel kind of fracture, which is evident by the adhered Al on the Ti fractured surface (Fig.8b). The fractured surface on the Al side (Fig. 8a) showcases the dimples, cleavage facets and tear edges, whereas the Ti side (Fig.8b) shows shallow dimples and the Al-rich zone (adhesion) is observed. With the increase in holding time, the fractured surfaces of the Al and Ti sides show a brittle type of failure, exhibiting salient fractography features. The shear and separation mechanism potentially exhibits additional dimples between the shallow dimples and the ridges. Separation typically presents sharp edges and demonstrates high contrast in the SEM images and moreover the absence of excess pores, slags, inclusions and poor welding areas signifies a quality welding [23-24]. Tab. 3 shows the EDS results for different points illustrated in Fig.8. The point EDS on the fractured surface primarily consists of Al with more than 90 at% signifying the formation of Al_3Ti intermetallic phase as it has less Gibbs free energy compared to other intermetallic phases like $AlTi_3$, $AlTi_2$, and AlTi. The inter solubility of the metals is also a key factor in diffusion welding. The solubility of the Al in Ti is almost 12 at%, whilst the solubility of the Ti in Al is only 0.12 at% [25], and this mainly affects the intermetallic formations and strength of the joints. The fractured surface on the Al side formed at 60 minutes (Fig.8c) exhibits tear ridges, step cleavages, and the crack initiation zone, whereas the fractured surface on the Ti side (Fig.8d) shows voids, cleavage facets and Al-rich zones. Furthermore, the fractured surfaces of joints formed at 90 (Fig.8 d-e) and 120 minutes (Fig.8 g-h) demonstrate inhomogeneous dimples, shallow dimples, inclusion, cleavage, and tear ridges.

The XRD analysis of the fractured surfaces further supports the identification of the actual intermetallic compounds formed at the joint interface. The XRD profile for the fractured surfaces formed at various holding times is shown in Fig. 9. The peaks at the Al fractured surfaces imply the presence of AlTi, Al_2Ti, and Al_3Ti, along with pure Al and Ti peaks. The fractured surface at the Ti side exhibits AlTi, Al_2Ti, and Al_3Ti, along with a pure Ti peak and does not show any Al peak, which strongly suggests the failure of the diffusion welded joints between the Al and intermetallic phase.

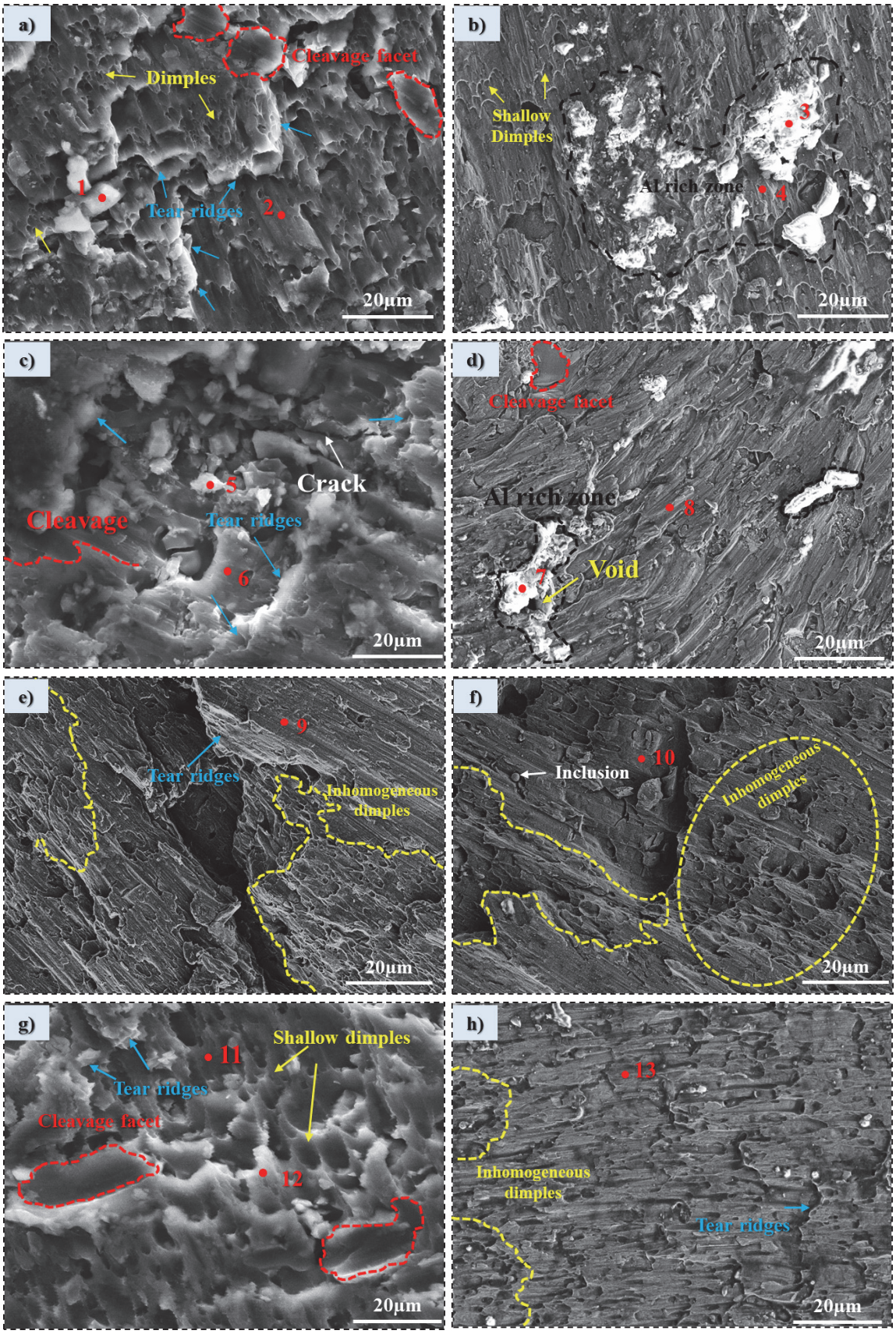

Figure 8: Fractography images of diffusion welded joints formed at various holding times (a, b) 30 min, (c, d) 60 min, (e, f) 90 min, (g, h) 120 min.

Point No.	Elements (at%)		
	Al	Ti	Cu
1	90.05	3.64	6.31
2	96.07	0.51	3.42
3	98.78	0.16	1.06
4	99.23	-	0.77
5	93.66	3.83	2.52
6	99.00	0.56	2.51
7	87.57	12.03	0.40
8	80.82	18.98	0.20
9	97.16	-	2.84
10	95.26	-	4.74
11	96.78	0.47	2.75
12	95.86	0.97	3.17
13	91.96	7.15	0.89

Table 3: EDS results on different points illustrated in Fig.8.

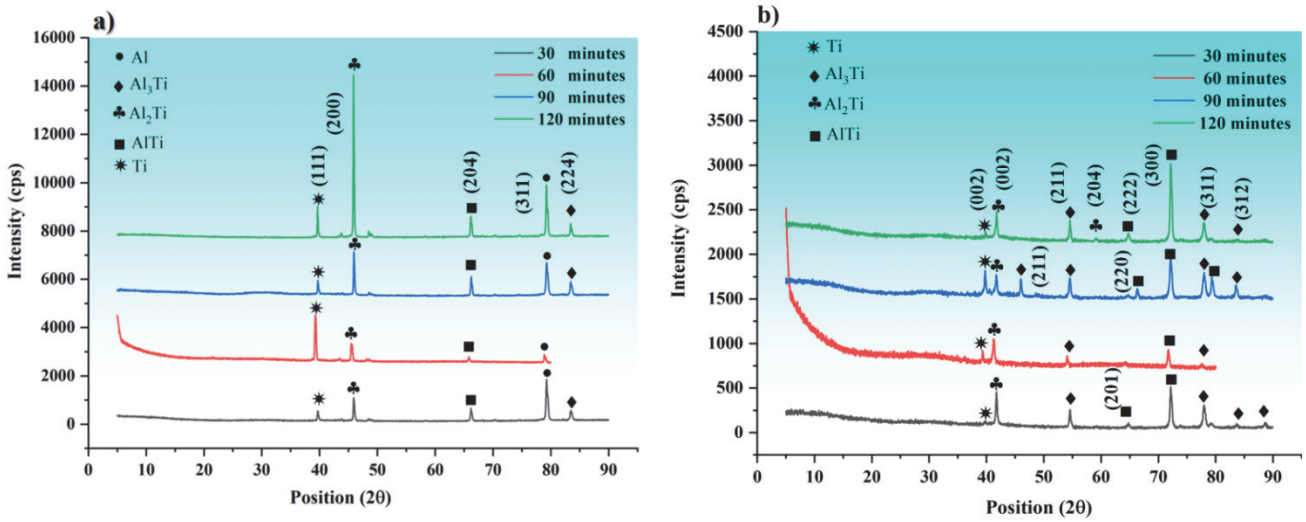

Figure 9: XRD profile for the fractured surfaces bonded at different holding times a) Al side b) Ti side.

CONCLUSIONS

- AA2219 and Ti-6Al-4V are diffusion welded for various holding times in the range of 30-120 minutes by keeping the bonding temperature and pressure constant.
- The hardness of the diffusion welded joints increased with the increase in holding time and attained a maximum hardness of 202.5 $HV_{0.05}$ for the joint formed at the holding time of 120 minutes.
- Maximum shear strength of 143.58 MPa is observed for the joint formed at 90 minutes and decreased when the holding time increased to 120 minutes due to the formation of thick intermetallic, which undeniably exhibits nonlinearity between the holding time and the bonding strength.
- The joints predominantly failed between Al and the reaction layer formed towards the Ti side, ensuring the brittle type of failure.
- The fractured surfaces on the Al and Ti sides illustrate the primary features like dimples, cleavage, cracks, voids and tear ridges.

CONFLICTS OF INTEREST

The authors declares no conflict of interest.

ACKNOWLEDGEMENT

This work was supported by the Research Promotion Scheme (RPS) AICTE, New Delhi. Grant Number: File No. 8-114/FDC/RPS (Policy-1)/2019-20. The support is greatly acknowledged by the authors

REFERENCES

[1] Trisolini, M., Lewis, H.G. and Colombo, C. (2016). Demise and survivability criteria for spacecraft design optimization. Journal of Space Safety Engineering, 3(2), pp.83-93.N.
[2] Norman, A., Bernad, A. and Resch, S. (2015). Development of aluminium-titanium tube joints for space propulsion systems. In 6th European Conference For Aeronautics And Space Sciences (EUCASS).
[3] Brassington, W.D.P. and Colegrove, P.A. (2017). Alternative friction stir welding technology for titanium–6Al–4V propellant tanks within the space industry. Science and Technology of Welding and Joining, 22(4), pp.300-318.
[4] Zavadski, A. (2018). Advanced welding technologies used in aerospace industry.
[5] Wei, Y., Li, J., Xiong, J., Huang, F., Zhang, F. and Raza, S.H. (2012). Joining aluminum to titanium alloy by friction stir lap welding with cutting pin. Materials characterization, 71, pp.1-5.
[6] Baqer, Y.M., Ramesh, S., Yusof, F. and Manladan, S.M. (2018). Challenges and advances in laser welding of dissimilar light alloys: Al/Mg, Al/Ti, and Mg/Ti alloys. The International Journal of Advanced Manufacturing Technology, 95, pp.4353-4369.
[7] Bi, Z.X., Li, X.J., Zhang, T.Z., Wang, Q., Rong, K., Dai, X.D. and Wu, Y. (2022). Microstructure and characterization of Ti–Al explosive welding composite plate. The International Journal of Advanced Manufacturing Technology, 123(5), pp.1825-1833.
[8] Vatnalmath, M., Auradi, V., Murthy, B.V., Nagaral, M., Pandian, A.A., Islam, S., Khan, M.S., Anjinappa, C. and Razak, A. (2023). Impact of bonding temperature on microstructure, mechanical, and fracture behaviors of TLP bonded joints of Al2219 with a Cu interlayer. ACS omega, 8(29), pp.26332-26339.
[9] Li, W. and Patel, V. (2022). Solid state welding for fabricating metallic parts and structures. DOI: 10.1016/B978-0-12-819726-4.00012-0
[10] Masahashi, N. and Hanada, S. (2005). Effect of pressure application by HIP on microstructure evolution during diffusion bonding. Materials transactions, 46(7), pp.1651-1655.
[11] Thiyaneshwaran, N., Sivaprasad, K. and Ravisankar, B. (2021). Characterization based analysis on TiAl3 intermetallic phase layer growth phenomenon and kinetics in diffusion bonded Ti/TiAl3/Al laminates. Materials Characterization, 174, p.110981.
[12] Rajakumar, S. and Balasubramanian, V. (2016). Diffusion bonding of titanium and AA 7075 aluminum alloy dissimilar joints—process modeling and optimization using desirability approach. The International Journal of Advanced Manufacturing Technology, 86, pp.1095-1112.
[13] Wei, Y., Aiping, W., Guisheng, Z. and Jialie, R. (2008). Formation process of the bonding joint in Ti/Al diffusion bonding. Materials Science and Engineering: A, 480(1-2), pp.456-463.
[14] Akca, E. and Gursel, A. (2017). The effect of diffusion welding parameters on the mechanical properties of titanium alloy and aluminum couples. Metals, 7(1), p.22.
[15] Jiangwei, R., Yajiang, L. and Tao, F. (2002). Microstructure characteristics in the interface zone of Ti/Al diffusion bonding. Materials Letters, 56(5), pp.647-652.
[16] Rusnaldy, R. (2001). Diffusion bonding: an advanced of material process. Rotasi, 3(1), pp.23-27.
[17] Luo, J.G. and Acoff, V.L. (2000). Interfacial reactions of titanium and aluminum during diffusion welding. Welding Journal -New York-, 79(9), pp.239-s.

[18] Liu, Z.W., Rakita, M., Han, Q., Li, J.G. (2012). A Developed Method for Fabricating In-Situ TiC p/Mg Composites by Using Quick Preheating Treatment and Ultrasonic Vibration. Metallurgical and Materials Transactions A. 43, pp. 2116-2124.
[19] Schuster, J.C. and Palm, M. (2006). Reassessment of the binary aluminum-titanium phase diagram. Journal of phase equilibria and diffusion, 27, pp.255-277.
[20] Ravisankar, B., Krishnamoorthi, J., Ramakrishnan, S.S. and Angelo, P.C. (2009). Diffusion bonding of SU 263. Journal of materials processing technology, 209(4), pp.2135-2144.
[21] Dai, J., Jiang, B., Zhang, J., Yang, Q., Jiang, Z., Dong, H. and Pan, F. (2015). Diffusion kinetics in Mg-Cu binary system. Journal of Phase Equilibria and Diffusion, 36, pp.613-619.
[22] Gietzelt, T., Toth, V. and Huell, A. (2018). Challenges of diffusion bonding of different classes of stainless steels. Advanced Engineering Materials, 20(2), p.1700367.
[23] Maruschak, P., Konovalenko, I. and Sorochak, A. (2023). Methods for evaluating fracture patterns of polycrystalline materials based on the parameter analysis of ductile separation dimples: A review. Engineering Failure Analysis, p.107587.
[24] Kryzhanivskyy, Y., Poberezhny, L., Maruschak, P., Lyakh, M., Slobodyan, V. and Zapukhliak, V. (2019). Influence of test temperature on impact toughness of X70 pipe steel welds. Procedia Structural Integrity, 16, pp.237-244.
[25] Wan, Q., Li, F., Wang, W., Hou, J., Cui, W. and Li, Y. (2021). Microstructure and properties of in situ Ti–Al intermetallic compound-reinforced Al matrix composites with dispersive distribution of core–shell-like structure. Composites and Advanced Materials, 30, p.26349833211006117.